

## Measurement of electric discharge machining bearing currents in brush-less direct-current motors

**Abstract.** The paper deals with electric discharge machining bearing currents in brush-less direct-current electric motors. The shunt resistor as a current sensor was analyzed regarding appropriateness for measurement of high-frequency bearing currents. The circuit model of electric discharge machining current's circuit was built to determine the influence of insulation sleeves and bypass bridge to the initial system. Parameters of the model were estimated with simplex algorithm. The measurements and investigations of bearing-currents' trend line were performed.

**Streszczenie.** Artykuł dotyczy zagadnienia prądów występujących przy elektrycznym rozładunku maszynowym (ang. Electrical Discharge Machining) w łożyskach bezszczotkowej maszyny DC. Rolę czujnika prądu spełnił równolegle dołączony rezystor. W celu określenia wpływu tulei izolacyjnych oraz bocznika na warunki początkowe, dokonano analizy modelu zjawiska. Stworzono obwód elektryczny, którego odpowiednie parametry estymowano przy pomocy algorytmu simpleksowego. Przedstawiono wyniki pomiarów i analiz. (Pomiary prądów elektrycznego wyładowania maszynowego w łożyskach bezszczotkowej maszyny DC).

**Keywords:** bearing currents, trend line, current sensor, equivalent circuit model.

**Słowa kluczowe:** prądy łożyskowe, linia trendu, czujnik prądu, obwód równoważny.

### Introduction

Bearing currents are parasitic phenomena, especially prominent in electric motors, supplied by inverters, like brush-less direct-current (BLDC) motors. Bearing life could be significantly reduced due to flow of electric current. Inverter-induced bearing currents can be divided into four groups, namely capacitive currents, electric discharge machining (EDM) currents, high-frequency circulating currents and bearing currents, due to currents between the motor and the load [1]. In low-power motors EDM currents are especially prominent, therefore this paper focuses on them.

Shaft voltage builds up in motor due to common mode voltage, introduced by inverter and stray capacitances in motor. Rotor and shaft of the motor are insulated from motor frame only with thin layer of bearing grease. If shaft voltage exceeds the value of threshold voltage, the thin grease layer is broken down and EDM current occurs [2].

Bearing currents cannot be measured directly by placing the current sensor into the bearing. Therefore motor needs insulated bearings and bypass bridge around the insulation (Fig. 2), which makes the measurement possible [3]. However insulation sleeve and bypass bridge change the initial electrical conditions in the bearing-current circuit. The change of electrical properties will be described further in this paper.

Because of high-frequency of EDM currents, special care considering current sensor is required. Typical sensors, used for bearing-current measurement are: shunt resistor, oscilloscope current probe and Rogowski coil. Current sensor needs suitably high bandwidth and its influence to the initial electrical conditions in bearing-currents' circuit has to be as low as possible. In this paper electrical properties and frequency response of current-sensing (shunt) resistor are analyzed. It is important that stray capacitances and inductances of the resistor are as low as possible and known.

Bearing currents were measured with previously analyzed shunt resistor. Shaft voltage was also measured. Parameters of bearing-currents' circuit between motor shaft and motor frame were estimated. Simplex algorithm was used for parameter estimation. Inputs for the estimation were measured shaft voltages and bearing currents.

Measurement and analysis of bearing-currents' trend line during half-hour test were performed and bearing endangerment was estimated.

### Analysis of current sensor

There are three main types of current sensors for bearing-current measurement, as it was described in previous chapter. Bandwidths of Rogowski coils are not sufficient for measurement of EDM currents. Good-quality high-frequency current probes were not available for us, therefore we have chosen current-sensing resistor with high bandwidth as a current sensor. Real resistor has both stray capacitance and stray inductance, which define resistor's frequency response and bandwidth. Equivalent circuit of real resistor was therefore modeled as serial connection of resistance and inductance and parallel connection of capacitance (Fig. 1b).

Resistance  $R_S$  in Fig. 1b denotes nominal resistance of resistor, whereas capacitance  $C_S$  and inductance  $L_S$  denote stray parameters. Values of stray capacitance and inductance were estimated with simplex algorithm from measured shaft voltage and bearing current, which is described later in this paper.

Resistance of shunt resistor is subject of compromise between influence that resistor provides to the initial system and influence of stray inductance to the impedance of real resistor. Low resistance is desired because of low influence on the initial system, whereas high resistance is desired to minimize the effect of stray inductance of the sensor.  $3\Omega$  resistor showed the best results in tests of different resistors.

Known values of real-resistor's parameters allow calculation of its frequency response according to (1).  $R_S$ ,  $L_S$  and  $C_S$  denote resistance, stray inductance and stray capacitance of real resistor, respectively.  $Z$  denotes impedance of real resistor,  $\omega$  angular frequency and  $\omega_0$  natural resonance angular frequency of the circuit.

$$(1) \quad \underline{Z}(\omega) = \frac{R_S + j\omega L_S}{1 - \omega^2 / \omega_0^2 + j\omega R_S C_S}; \omega_0 = \frac{1}{\sqrt{L_S C_S}}$$

Correction algorithm that enables correction of measured signal, distorted due to limited bandwidth of current sensor, can be derived by using (1). Measured signal is transformed to frequency spectrum and multiplied by inverse function of frequency response of real resistor. Frequencies, higher than the highest frequency of the signal of interest (approximately 40MHz), have to be excluded

from the correction, otherwise high-frequency noise is significantly amplified.

### Bearing-currents' circuit model and parameter estimation

Bearing could be modeled as capacitor in bearing-current circuit, when motor speed is higher than few hundred rotations per minute [1]. During low-speed operation and during discharge in bearing, bearing shows conductive properties. Therefore bearing is commonly modeled with serial connection of resistor, inductor and switch and with parallel connected capacitor as it is shown in Fig. 1a.

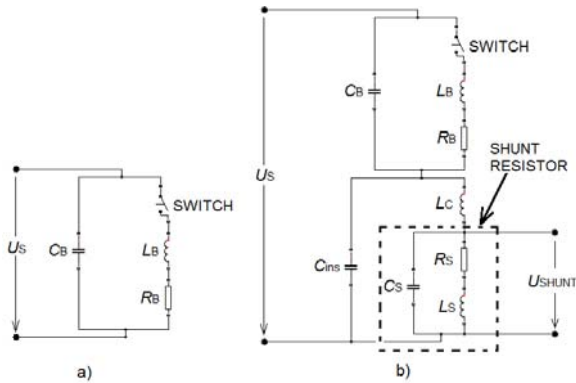


Fig. 1. Equivalent circuit of bearing: a) bearing; b) bearing, insulation sleeve and bypass bridge with current sensor.

Switch simulates moments, when bearing shows conductive properties. With bearing insulation and bypass bridge, additional impedance is inserted into bearing-currents' circuit between the shaft and the frame (Fig. 2). The scheme of the whole equivalent circuit is shown in Fig. 1b. This circuit allows the analysis of influence that insulation sleeve and bypass bridge have to initial system.  $C_B$ ,  $L_B$  and  $R_B$  denote bearing capacitance, inductance and resistance, respectively.  $C_{ins}$  is capacitance of insulation sleeve,  $L_C$  inductance of cooper wire (bypass bridge) and  $C_S$ ,  $L_S$  and  $R_S$  are capacitance, inductance and resistance of shunt resistor, respectively. Approximate level of parameters was estimated by calculation of capacitances and inductances, using analytical formulas. These values were used in simplex algorithm to find the optimal values of the parameters, considering measured shaft voltage and voltage drop on shunt resistor. Simplex algorithm was performed on the model shown in Fig. 1b. To obtain robust values of parameters, 15 measurements with different values of shaft voltage and voltage drop on shunt resistor were used in parameter-estimation algorithm (simplex algorithm). The final values of the parameters are the average of parameter values from all 15 estimations.

The shape of EDM bearing current is damped sinus. This is due to oscillating properties of the circuit during discharge. Electrical parameters of bearing itself ( $C_B$ ,  $L_B$  and  $R_B$ ) are not constant during the discharge, because of rather complex mechanical characteristics of bearing - phenomena of Hertz contact and lubricating-grease film. This is reflected in variable frequency of EDM current during discharge. To consider the change of the bearing parameters in parameter-estimation algorithm, each measured signal was divided into five sections, where each section comprised one period of EDM current. First period of the current is the most prominent one and therefore it was used in simplex algorithm [8] to estimate all the parameters of the model (Fig. 1b). For every other period only bearing parameters ( $C_B$ ,  $L_B$  and  $R_B$ ) were estimated. Other

parameters were fixed to the value, found by simplex algorithm, using the first period of the current.

The model with parameters, estimated by simplex algorithm, was validated on additional 15 measurements of shaft voltage and voltage drop on shunt resistor. The error of the simulated signal, compared to the measurement, was defined as a sum of squared errors (2) and as an error of peak value of EDM current (3).  $f_i$  and  $\hat{f}_i$  denote measured value and simulated value of  $i$ -th sample, respectively.

$$(2) \quad SSE = \frac{\sum (f_i - \hat{f}_i)^2}{\sum (f_i)^2}$$

$$(3) \quad ERR = \frac{\max(|f_i|) - \max(|\hat{f}_i|)}{\max(|f_i|)}$$

### Measurement of EDM bearing currents

All measurements were performed on 1.6kW BLDC motor with star winding type. Motor had bearings insulated from motor frame (Fig. 2). Bypass bridge was installed over the insulation of one bearing. Digital signal oscilloscope was used as measurement equipment. 3Ω shunt sensor was used for current sensing and microfiber shaft probe (brush) to measure the shaft voltage. The scheme of the measurement system is shown in Fig. 2. All measurements were performed in no-load condition at nominal speed of the motor.

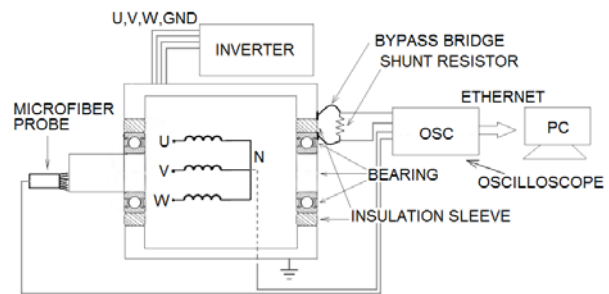


Fig. 2. Scheme of measurement system

Common mode voltage, shaft voltage and voltage drop on shunt resistor (bearing current) were measured during first group of measurements. Common mode voltage and shaft voltage were measured regarding to motor frame. Capacitive and EDM currents could be distinguished by observing the common mode voltage and shaft voltage. Capacitive current occur during transition of the common mode voltage. The shape of shaft voltage tracks the shape of common mode voltage. EDM current could occur at any time, when shaft voltage is higher than bearing threshold voltage. However the value of bearing threshold voltage significantly changes during bearing rotation. Shaft voltage quickly drops to 0 during EDM current occurrence and does not track the shape of common mode voltage in this time.

Shaft voltage and voltage drop on shunt resistor (bearing current) were measured to estimate the parameters of EDM-currents' circuit. Currents with different amplitudes were measured, which provide better parameter estimation.

Bearing voltage ratio ( $BVR$ ) was calculated from measurements of common mode voltage and shaft voltage just after the motor startup (when EDM currents do not occur).  $BVR$  is defined with (4), and denotes how much of common mode voltage is coupled to the shaft.  $u_{SH}$  is shaft voltage and  $u_{CM}$  common mode voltage.

$$(4) \quad BVR = \frac{u_{SH}}{u_{CM}}$$

More detailed view of trend line of bearing currents gave half-hour test. Motor run at nominal speed and with no-load for half an hour and only bearing currents were measured during this period. Peak values of bearing currents were used as a measure of level of bearing endangerment. Half-hour test allowed the observation of bearing currents in bearing-temperature steady state. It is not possible to detect every bearing current that occurs during half-hour test. This would require large amount of oscilloscope's memory, because of high sampling frequency and long measurement time. However it is also not necessary. To determine the trend line it is enough to detect approximately one bearing current per second, even though much more discharges occur in this time. The same test was repeated after 24h of motor operation.

### Results

Electrical parameters of the circuit in Fig. 1b were estimated with parameter estimation method (simplex algorithm), using 15 independent measurements of shaft voltages and voltages on shunt resistor. Table 1 shows average values of estimated parameters. Bearing parameters ( $C_B$ ,  $L_B$  and  $R_B$ ) are different in every period of bearing current, whereas the other parameters are constant for all periods and are therefore written only for the first period.

Table 1. Parameters of EDM-current equivalent circuit obtained with parameter-estimation method. Bearing parameters are estimated for each period of EDM current.

|                    | 1. per.              | 2. per.              | 3. per.              | 4. per.              | 5. per.              |
|--------------------|----------------------|----------------------|----------------------|----------------------|----------------------|
| $C_b$ [F]          | $6,0 \cdot 10^{-10}$ | $4,6 \cdot 10^{-10}$ | $2,8 \cdot 10^{-10}$ | $1,2 \cdot 10^{-10}$ | $1,1 \cdot 10^{-11}$ |
| $L_b$ [H]          | $6,1 \cdot 10^{-16}$ | $4,7 \cdot 10^{-16}$ | $2,2 \cdot 10^{-16}$ | $1,2 \cdot 10^{-16}$ | $1,9 \cdot 10^{-16}$ |
| $R_b$ [ $\Omega$ ] | 8,5                  | 14,6                 | 42,6                 | 109,7                | $2,4 \cdot 10^4$     |
| $C_{ins}$ [F]      | $4,4 \cdot 10^{-11}$ |                      |                      |                      |                      |
| $L_c$ [H]          | $7,6 \cdot 10^{-9}$  |                      |                      |                      |                      |
| $C_s$ [F]          | $1,1 \cdot 10^{-9}$  |                      |                      |                      |                      |
| $L_s$ [H]          | $1,4 \cdot 10^{-9}$  |                      |                      |                      |                      |
| $R_s$ [ $\Omega$ ] | 3,0                  |                      |                      |                      |                      |

According to parameter values of shunt resistor in Table 1 and to (1) the bandwidth of shunt resistor is sufficiently high, because natural resonance frequency of the real resistor is 133MHz. That means that resonance frequency is significantly higher than frequency components of measured quantities. Therefore correction algorithm, explained in section "Analysis of current sensor" is not required.

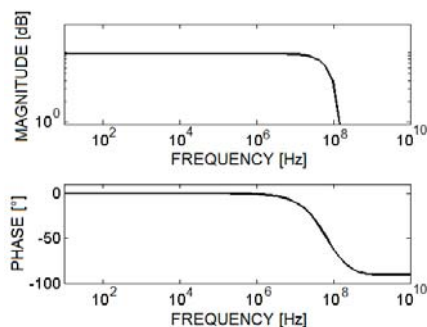


Fig. 4. Frequency response of used shunt resistor (amplitude and phase spectrum)

Measured voltage on shunt resistor has to be only divided by value of resistance  $R_S$  to calculate the EDM current. Frequency response of shunt resistor is shown in Fig. 4.

Parameters from Table 1 were validated, using 15 additional measurements of shaft voltage and voltage on shunt resistor to calculate difference between measured and simulated signal. Table 2 shows average error and standard deviation of the error, obtained during validation. Errors  $SSE$  and  $ERR$  are defined with (2) and (3), respectively.

Table 2. Average error of 15 simulated signals, obtained within validation process.  $SSE$  denotes "sum of square errors" and  $ERR$  denotes error of peak value of the signal.

|                        | $SSE$ | $ERR$ |
|------------------------|-------|-------|
| Average of errors [%]  | 4,88  | 3,84  |
| Standard deviation [%] | 2,34  | 11,05 |

Both errors are under 5%. Sum of square errors has also low standard deviation. Average error of bearing-current peak value is lower than sum of square errors, but has much higher standard deviation. Figure 5 shows example of measured and simulated EDM current.

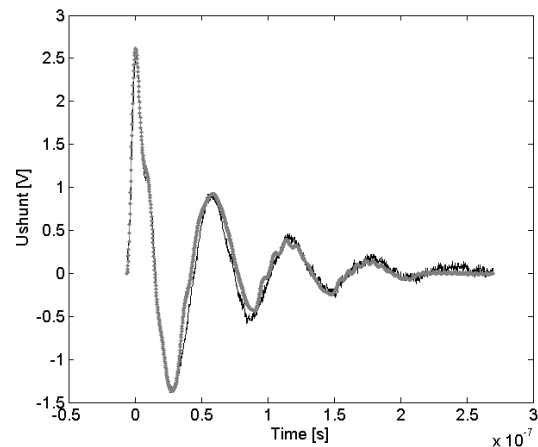


Fig. 5. Comparison of measured quantity (dark curve) and simulated quantity (bright curve)

Signals are almost identical in the first period, whereas there are minor deviations in the following periods.

Only capacitive bearing currents occur just after motor startup, because the temperature of bearing grease is still low and therefore the threshold bearing voltage is high. During this time it is possible to define  $BVR$  (4), because shaft voltage tracks the shape of common mode voltage. Value of  $BVR$  for the investigated motor is 3,7%.

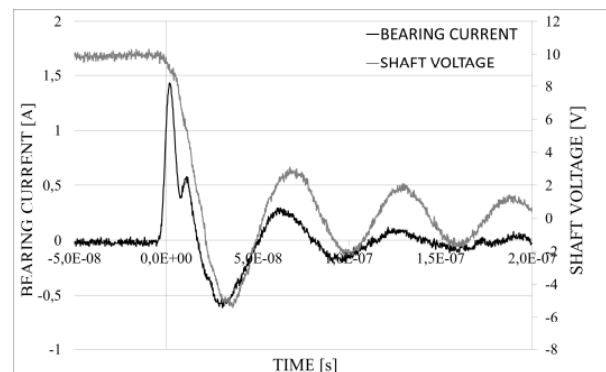


Fig. 7. Example of measured EDM current and shaft voltage

Example of EDM bearing current together with shaft voltage is shown in Fig. 7. EDM current has the shape of

damped sinus (dark curve). Shaft voltage (bright curve) rapidly drops to 0 with some oscillations during this time.

Peak values of bearing currents, detected during half-hour test are shown in Fig. 8 (every point denotes one bearing current). Peak values have low values for the first 15min after motor startup. Additional researches showed, that during this time mostly capacitive current occur. This is a consequence of low temperature of bearing grease and therefore high threshold bearing voltage. After 15min temperature in bearing rises and threshold bearing voltage drops approximately to the level of amplitude of the shaft voltage. Therefore EDM currents with high amplitudes are frequent. Later bearing temperature additionally rises and threshold bearing voltage additionally drops. EDM currents are therefore frequent, but have lower amplitudes. Dark bold curve denotes trend line of peak values of bearing currents, which is defined as moving average of 50 currents.

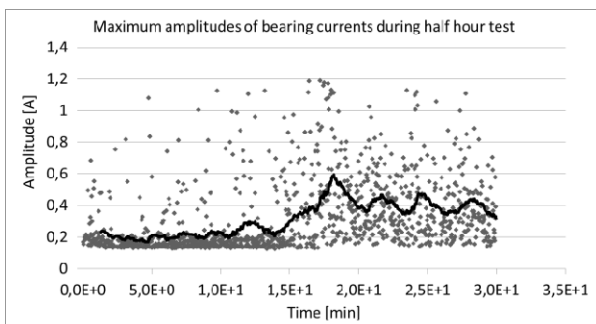


Fig. 8. Bearing currents, detected during half-hour test. Every point in graph denotes peak value of one bearing current.

The same half-hour test was repeated after 24h motor operation at nominal speed and no-load. Trend line of bearing currents measured in this test is shown in Fig. 9. Trend line (dark bold curve) has value around 0,2A in this case, whereas in test after motor startup it had values between 0,2A and 0,4A.

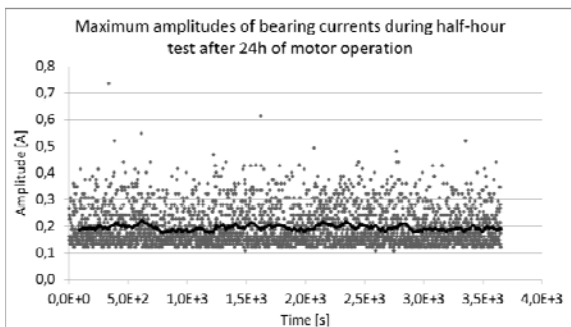


Fig. 9. Bearing currents, detected during half-hour test, performed after 24-hour motor operation. Every point in graph denotes peak value of one bearing current.

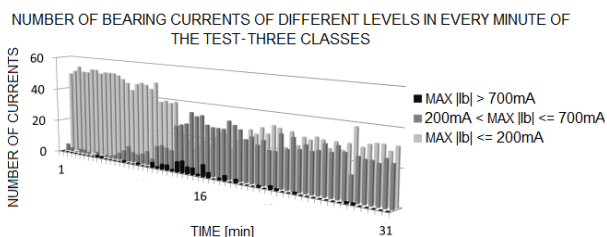


Fig. 10. Number of bearing currents of different levels, detected in every minute of half-hour test. The test was performed just after motor startup.

Figure 10 shows number of bearing currents of different levels in every minute of the test. Currents are divided into three classes (currents with peak values lower than 200mA, currents with peak values between 200mA and 700mA and currents with peak values above 700mA).

## Conclusions

Limited bandwidth of current sensors and influence of insulation sleeves and bypass bridge regarding bearing currents were investigated in this paper. The analysis of current sensor showed that used sensor has appropriate bandwidth. Insulation sleeves and bypass bridge have some influence to initial system and therefore they have to be designed in a way that stray capacitances and inductances are as low as possible. Stray inductance in bearing during discharge is low and could be neglected. Proposed model of EDM-current circuit provide relatively good results and therefore can be used for further analyses of bearing currents. Capacitive currents as well as EDM currents are present in the investigated motor. Their peak levels, when temperature in bearing stabilizes, are mostly under 200mA. These levels are commonly considered as not dangerous to the bearings, but further investigations regarding bearing-current densities and dissipated energy should be also conducted.

## Acknowledgements

Operation part financed by the European Union, European Social Fund.

## REFERENCES

- [1] Muetze A., Binder A., Techniques for Measurement of the Parameters Related to Inverter-Induced Bearing Currents, *IEEE Transactions on Industry Applications*, 43 (2007), No. 5, 1274-1283
- [2] Muetze A., Binder A., Calculation of Motor Capacitances for Prediction of the Voltages Across the Bearings in Machines of Inverter-Based Drive Systems, *IEEE Transactions on Industry Applications*, 43 (2007), No. 3, 665-672
- [3] Iimori K., Shinohara K., Yamamoto K., Morigami A., Approaches to Suppressing Shaft Voltage in Brushless DC Motor Driven by PWM Inverter, *Electrical Engineering in Japan*, 166 (2009), No. 4, 406-411
- [4] Gulez K., Adam A.A., High-Frequency Common-Mode Modeling of Permanent Magnet Synchronous Motors, *IEEE Transactions on Electromagnetic Compatibility*, 50 (2008), No. 2, 423-426
- [5] Magdun O., Gemeinder Y., Binder A., Prevention of harmful EDM currents in inverter-fed AC machines by use of electrostatic shields in stator winding overhang, *IECON 2010 – 36th Annual Conference on IEEE Industrial Electronics Society*, 962-967, 2010
- [6] Magdun O., Binder A., Calculation of Roller and Ball Bearing Capacitances and Prediction of EDM Currents, *Industrial Electronics, 2009. IECON '09. 35th Annual Conference of IEEE*, 1051-1056, 2009
- [7] Maki-Ontto P., Luomi J., Induction Motor Model for the Analysis of Capacitive and Induced Shaft Voltages, *2005 IEEE International Conference on Electric Machines and Drives*, 1653-1660, 2005
- [8] Matlab Documentation, [online]: <http://www.mathworks.com/help/techdoc/>

**Authors:** Gregor Vidmar, Domel, d.o.o., Otoki 21, 4228 Železniki, E-mail: [gregor.vidmar@domel.si](mailto:gregor.vidmar@domel.si); Jurij Pfaifar, E-mail: [jure.pfaifar@domel.si](mailto:jure.pfaifar@domel.si); izr. prof. dr. Dušan Agrež, E-mail: [dusan.agrez@fe.uni-lj.si](mailto:dusan.agrez@fe.uni-lj.si); izr. prof. dr. Damijan Miljavec, University of Ljubljana, Faculty of electrical engineering, Tržaška 25, 1000 Ljubljana, E-mail: [miljavec@fe.uni-lj.si](mailto:miljavec@fe.uni-lj.si).